Arabian Journal of Chemistry (2020) **13**, 8815–8823

King Saud University

Arabian Journal of Chemistry

www.ksu.edu.sa
www.sciencedirect.com

ORIGINAL ARTICLE

Identification of active chemical constituents of *Asplenium ruprechtii* Sa. Kurata based on *in vitro* neuroprotective activity evaluation

Zhi-Bo Jiang [a,b], Xing Lu [a], Jing-Zhi Chen [a], Xiao-Li Ma [a,b], Yi-Hu Ke [a,b], Xin Guo [a,b], Hai Liu [a,b], Chong-Long Li [a,b,*], Fang Wang [c,*], Xiu-Li Wu [d,*], Dai-Zhou Zhang [c], Shuang Cao [e]

[a] *Department of Pharmaceutical Engineering, School of Chemistry and Chemical Engineering, North Minzu University, Yinchuan 750021, PR China*
[b] *Key Laboratory of Chemical Engineering and Technology of State Ethnic Affairs Commission, North Minzu University, Yinchuan 750021, PR China*
[c] *Shandong Academy of Pharmaceutical Sciences, Jinan 250101, PR China*
[d] *College of Pharmacy, Ningxia Medical University, Yinchuan 750004, PR China*
[e] *Key Laboratory for Green Chemical Process of Ministry of Education, School of Chemical Engineering and Pharmacy, Wuhan Institute of Technology, Wuhan 430072, PR China*

Received 4 August 2020; accepted 4 October 2020
Available online 15 October 2020

KEYWORDS

Asplenium ruprechtii;
Neuroprotective activity;
Chemical constituents;
9,19-Cycloartane-triterpenoid saponins;
Structural determination

Abstract Mining structural novel and bioactive natural products from traditional Chinese drugs and folk medicines have attracted attention from pharmacologists and pharmaceutical chemists for a long time. In this study, the chemical constituents of *Asplenium ruprechtii* Sa. Kurata was systematically studied based on the evaluation of neuroprotective activity on hydrogen peroxide (H_2O_2)-induced damage of SH-SY5Y cell lines. Sixteen chemical monomers (**1**–**16**), including two new structures of 9,19-cycloartane-triterpenoid saponins (**1**,**2**), were discovered. Their chemical structures were established based on extensive spectroscopic data analysis, including the one- and two-dimensional (1D and 2D) nuclear magnetic resonance (NMR) data and high-resolution electrospray ionization mass spectrometry (HRESIMS). All monomer compounds were docked with an "active pocket" at the N-terminal of the GluN2B protein, where compounds **13**–**16** were found to possess high binding scores, which warrant further study on the molecular mechanism. Our

* Corresponding authors at: Department of Pharmaceutical Engineering, School of Chemistry and Chemical Engineering, North Minzu University, Yinchuan 750021, PR China (C.-L. Li). Institute of Traditional Chinese Medicine, Shandong Academy of Pharmaceutical Sciences, Jinan 250101, PR China (F. Wang).
E-mail addresses: chlong@nun.edu.cn (C.-L. Li), wangfang_84@163.com (F. Wang), wu.xiuli2005@163.com (X.-L. Wu).

Peer review under responsibility of King Saud University.

Production and hosting by Elsevier

https://doi.org/10.1016/j.arabjc.2020.10.011

findings provide insight and research techniques for discovering new drugs based on neuroprotective activity.

1. Introduction

Screening novel structures and bioactive entities have become one of the most important methods for discovering clinical drugs. Statistics show that over 50% of clinical drugs come directly from natural products or their derivatives (Huang et al., 2019; Jamzivar et al., 2019; Treml et al., 2020). Traditional Chinese medicine and folk drugs have become important sources for drug development due to their long history (thousands of years) of safe use and systematic medication experience. With the development of modern separation methods and technologies, thousands of compounds have been separated from natural resources annually, including hundreds of new structural entities (Caputo et al., 2020). Because there are few compounds with good biological bioactivity, systematic and in-depth study of biological activities remains essential. Separation of compounds without the guidance of biological activity increases the probability of repeated discovery. Each year, over 500 compounds are reported repeatedly either in the same or different species (Newman and Cragg, 2020). Therefore, the construction of activity-mediated separation of bioactive molecules has become one of the hotspots in natural products research.

Asplenium ruprechtii Sa. Kurata, previously named *Comptosorus sibiricus* rupr., is widely distributed in the north of China, Korea, Japan, and the Far East of Russia. The whole plant has been used to treat severe endometrorrhagia, bleeding wound, and Buerger's disease in clinical practice or folk use (Ching, 1978; Christenhusz et al., 2011; Christenhusz and Chase, 2014; Hasebe et al., 1995; Lin and Ronald, 2013). The early research, led by Shenyang Pharmaceutical University, showed that the plant that was collected from Northeast China was rich in triterpenoid saponin, flavonoid glycoside, and phenolic and organic acids (41K of Shenyang College of Pharmacy, 1977; Yang et al., 2012). Our previous study on the activity of total flavonoids from the large polar parts of *A. ruprechtii* collected in Henan province of China on thromboocclusive vasculitis model rats showed that total flavonoids dilated peripheral blood vessels and could block α receptors and excitatory β receptors, relieve vasospasm of skin and mucous membrane, and improve the overall blood circulation of diseased limbs (Liang et al., 2011). In addition, we discovered over 40 compounds in continuous chemical constituent studies, including a novel skeleton of *C*-stiryl iridoid glycoside and five new cycloartane glycosides (Liang et al., 2017; Noh and Ismail, 2020; Vieira et al., 2016; Wang et al., 2020; Wang et al., 2019a, 2019b). However, these compounds could not fully represent the clinical efficacy of *A. ruprechtii*.

N-methyl-D-aspartic acid (NMDA) receptors are a class of ionic glutamatergic receptors, which control various glutamate synaptic communications (Zhou et al., 2013). GluN2B NMDA receptor in synapses can maintain active continuous cell communication. Multiple animal experimental evidence suggests that the NMDA receptor of GluN2B (GluN2B-NMDA receptor) induces excitotoxic cell death and amyloid-beta (Aβ) synaptic dysfunction (Li et al., 2010; Li et al., 2008; Liu et al., 2020). Therefore, the inhibition of the GluN2B-NMDA receptor is considered as a potential therapeutic strategy for Alzheimer's disease to provide neuroprotection and improve cognitive function. We established a method to evaluate the neuroprotective biological activity of extracts from traditional Chinese medicine and folk medicine using hydrogen peroxide (H_2O_2)-induced damage of SH-SY5Y cell lines as a model and found potential bioactivity in *A. ruprechtii* extract. Based on *in vitro* neuroprotective activity evaluation, the chemical constituents were investigated. Sixteen monomers (**1**–**16**, Fig. 1) were discovered and structurally characterized using extensive analysis of one- and two-dimensional (1D and 2D) nuclear magnetic resonance (NMR) data and high-resolution electrospray ionization mass spectrometry (HRESIMS). Herein, we report biological activity-mediated separation and structural identification and characterization.

2. Materials and methods

2.1. Chemicals and material

A. ruprechtii Sa. Kurata samples were collected in April 2017 from Yuzhou City, Henan Province, China. Plant identity was verified by Professor Qi Guo of Shandong Academy of Pharmaceutical Sciences, where a voucher specimen (No. 20160425) was deposited.

Anton Paar MCP 300 modular circular polarimeter (Anton Paar GmbH, Germany) was used to measure optical rotations. The NMR spectra of compounds **1** to **16** were acquired at 600 or 400 MHz for ^{1}H and 150 or 100 MHz for ^{13}C, respectively, using Bruker Avance AVIII-600 (or 400) spectrometer, and the references were standardized by solvent peaks. The HRESIMS data were measured using the LTQ Orbitrap XL instrument (Thermo Scientific, SanJose, CA, USA), while the high-performance liquid chromatography-tandem mass spectrometry (HPLC-MS/MS) data were acquired using the Agilent Q-TOF 6530 instrument (Agilent Technologies, Santa Clara, CA, USA). Silica gel (200–300 mesh, Qingdao Marine Chemical Inc. Qingdao, China) and Sephadex LH-20 (Pharmacia Biotech AB, Uppsala, Sweden) were used for column chromatography (CC). Semi-preparative HPLC separation was performed with the Shimadzu LC-10AT instrument with a refractive index detector (Shodex RI-201H; Shimadzu Corp., Tokyo, Japan), using a Shim-pack VP-ODS column (250 mm × 20 mm, 5 μm; Shimadzu Corp., Tokyo, Japan). The thin-layer chromatography (TLC) was performed with glass precoated silica gel GF254 plates (Qingdao Marine Chemical Inc.). Spots were visualized under ultraviolet (UV) light or by spraying with 7% sulphuric acid (H_2SO_4) in 95% ethanol alcohol (EtOH) followed by heating. Unless otherwise noted, all chemicals were obtained from commercially available sources and were used without further purification.

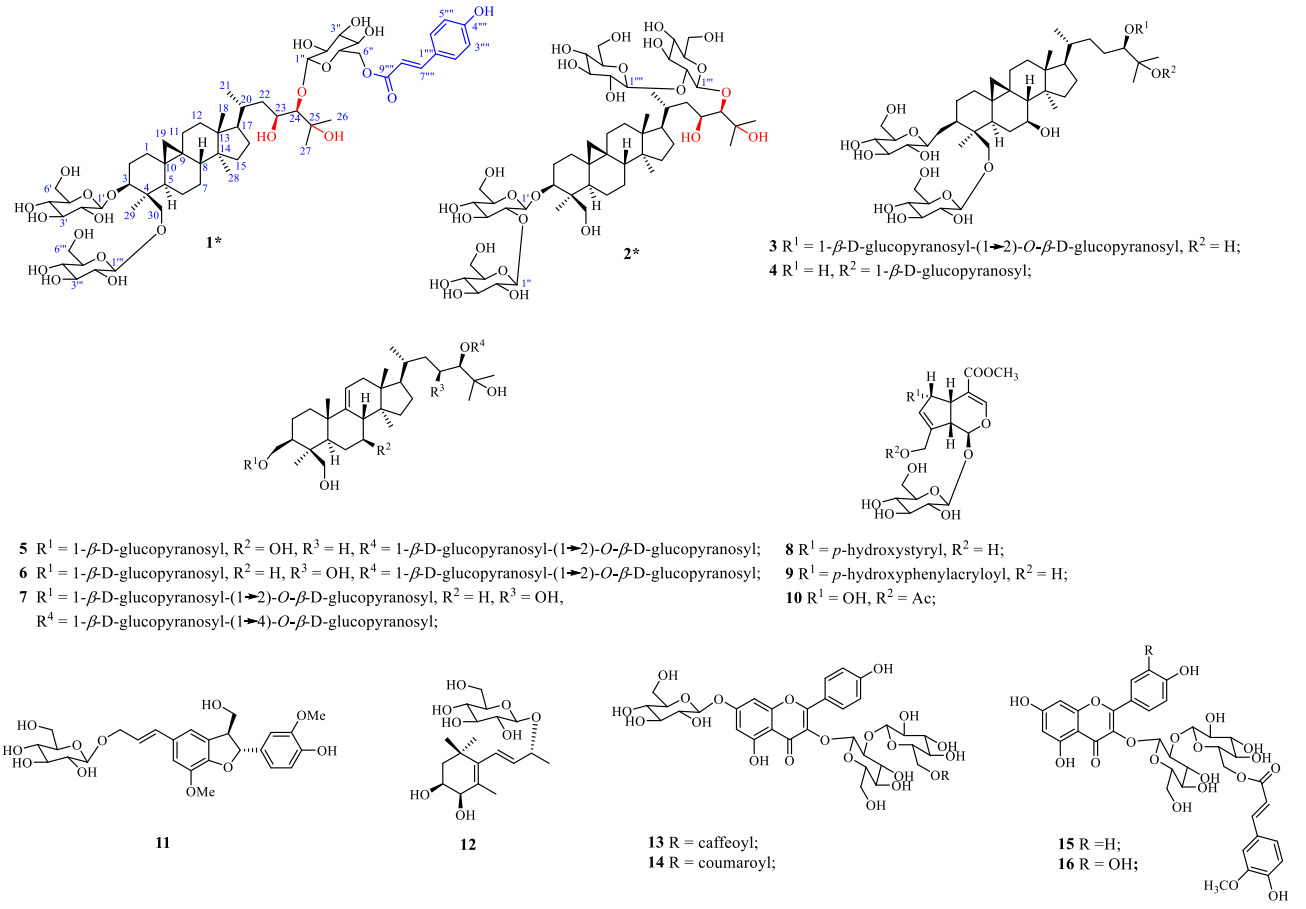

Fig. 1 Chemical structures of compounds **1**–**16**. New compounds **1** and **2** are assigned by asterisks (*).

2.2. Neuroprotective activity assay

2.2.1. SH-SY5Y cell culture

Human neuroblastoma SH-SY5Y cells were grown in T-75 flasks and incubated at 37 °C and 5% carbon dioxide (CO_2) in a humidified incubator. The completed media was composed of Dulbecco's Modified Eagle Medium (DMEM) + Ham's F-12 (1:1, Sigma Aldrich). When cells reached 80–90% confluency, they were subcultured. First, the culture medium was discarded and washed two times with phosphate-buffered saline (PBS) without calcium and magnesium ions. Then, 1.0 mL digestive solution (0.25% trypsin-0.53 mM EDTA) was added into the culture bottle, which was turned upside down and incubated at 37 °C for three minutes to preheat. The culture bottle was then over and allowed trypsin contact with the cell surface for about 30 s. Thereafter, the digestion of the cells was observed under the inverted microscope. Once most of the cells (over 80%) become round, they were quickly taken back to the operating table and a small amount of complete medium was added to terminate digestion. About 8.0 mL/bottle of the complete medium was added and then divided it into a new culture bottle.

2.2.2. Cell viability

SH-SY5Y cells were seeded at a density of 1×10^4 cells per well in clear 96-well cell culture plates. Different concentrations of H_2O_2 (50–250 μM) were freshly prepared before each experiment from a 30% stock solution and incubated at 37 °C with 5% CO_2 for 90 min.

The color rendering method was after Zhang et al. (2007). After 90 min exposure to H_2O_2, 10 μL of MTT (5 mg/mL in PBS) was added to each well and the cells were incubated for 60 min. After obtaining the supernatant, 60 μL of dimethyl sulfoxide (DMSO) was added to each well to dissolve the precipitate. The solution was measured at $\lambda = 570$ nm using a SpectraMax 190 Microplate Reader (Molecular Devices, San Jose, CA, USA). To the test group, samples were added in concentrations of 50 μg/mL for the crude extract and separation fragments and 10^{-5} M for the monomer compounds; a blank control was used for the control group.

2.3. Cytotoxicity assay

The cytotoxicity assay was performed following Zhang et al. (2008). The human cancer cell lines (HL-60 and HepG2) were maintained in Roswell Park Memorial Institute (RPMI)-1640 medium (Gibco, Life Technologies, Grand Island, NY, USA), supplemented with 10% of heat-inactivated bovine serum (Sijiqing Biomaterial, Hangzhou, China), 2 g/L of sodium bicarbonate ($NaHCO_3$), and 100 units/mL of both penicillin and streptomycin in humidified 5% CO_2 at 37 °C. Briefly, cells were seeded in 96-well tissue culture plates for 24 h, and then 100 μL of cell culture medium containing the test compounds dissolved in DMSO was added to the cells.

The cells were re-incubated with CO_2 for another 72 h with the various concentrations of the compounds. About 20 μL of cell counting kit-8 (CCK-8) solution (Dojindo Molecular Technologies, Japan) was added into the mixture and incubated for 2 h. The optical density at 450 nm was measured on a BioRad 550 instrument (BioRadLaboratories, Hercules, CA, USA). All compounds were tested at five concentrations (50, 5, 0.5, 0.05, and 0.005 μM/mL) in triplicate, with Sorafeni used as a positive reference.

2.4. Extraction and isolation

The air-dried whole herbs of *A. ruprechtii* (17.4 kg) were extracted with 11.0 L of 95% EtOH at room temperature for 3 × 48 h. The ethanol extract was evaporated under reduced pressure to yield a dark brown residue (528.6 g), which was suspended in water (H_2O) (1.5 L) and partitioned with ethyl acetate (EtOAc, 6 × 1 L). The aqueous phase (GSJ-M) was applied to an AB-8 macroporous adsorbent resin (1000 g) column and eluted successively with H_2O (GSJ-M-A), 30% EtOH (GSJ-M-B), 50% EtOH (GSJ-M-C), and 95% EtOH (GSJ-M-D) (5000 mL each), to yield four corresponding fractions GSJ-M-A-D. After removing the solvent under reduced pressure, fraction GSJ-M-C (73.9 g) was separated by CC over MCI gel CHP 20P (1 L), with successive elution using H_2O (2 L), 15% EtOH (3 L), 30% EtOH (3 L), 70% EtOH (3 L), and 95% EtOH (2 L), to give fractions GSJ-M- C1 to GSJ-M-C5. Fraction GSJ-M-C4 (10.3 g) was subjected to CC over silica gel, eluting with a gradient of increasing 95% EtOH concentration (0–50%) in EtOAc, to yield fractions GSJ-M-C4-1 to GSJ-M-C4-3 based on TLC analysis. Fraction GSJ-M-C4-3 (3.6 g) was separated via reverse-phase medium-pressure liquid chromatography (RP-MPLC) eluting with a gradient of MeOH (0–100%) in H_2O, and then purified by RP-HPLC (27% MeOH in H_2O) to give **1** (33.3 mg), **2** (14.3 mg), and **10** (103.4 mg), respectively. Fraction GSJ-M-C4-2 (7.5 g) was subjected over Sephadex LH-20 (CH_2Cl_2/MeOH, 1:1), and then purified by RP-HPLC (25% MeOH in H_2O) to obtain compounds **13** (5.72 mg), **14** (2.49 mg), **15** (33.5 mg), and **16** (173.3 mg), respectively. The isolation and purification progress for compounds **3** to **7** see Wang et al. (2020) and **8**, **9**, **11**, **12** see Wang et al. (2019a, 2019b).

2.5. Docking procedure

Molecular docking was implemented using the surflex-docking package of Sybyl-X 2.1. A cocrystal structure of the heterodimer of the GluN1b-GluN2B NMDA receptor in which amino-terminal domains bind to allosteric inhibitor 93-31 (6E7U) was obtained from the Protein Data Bank (PDB). Before docking, 6E7U was prepared by removing water and magnesium ions and extracting the ligand. The addition of hydrogen and charges and treatment of the terminal residues were also performed on 6E7U. Then "protomol" was generated using the ligand-based mode and an appropriate binding pocket was formed. The reliability of the surflex-docking was validated by re-docking the original ligand into the binding pocket. Next, all the candidate compounds were docked into the binding pocket and 20 possible docked conformations were obtained with different scores.

2.5.1. Results and discussion

The whole plants of *A. ruprechtii* were extracted with 95% EtOH and the low polarity of the fat-soluble fraction and plant pigment was removed by extraction with acetic ether. Residual organic solvents in the aqueous phase were removed under reduced pressure and the water mixture was fragmented through AB-8 macroporous adsorbent resin.

All intermediate fragments were evaluated for their potential neuroprotective effect on cell viability of H_2O_2-induced apoptosis in SH-SY5Y. We found that after elution with 50% EtOH, the viability of SH-SY5Y cell lines was 77.10%, which was 15.5% higher than the negative control (Table 1). This implied that compounds in 50% EtOH elution might possess neuroprotective activity. Therefore, the chemical compositions were systematically investigated, which yielded 16 monomers (Fig. 1). The structures of compounds **1** to **16** were determined by extensive spectroscopic data analysis. Structural characterization of compounds **2** to **7** and **8**, **9**, **11**, **12** have been reported in Wang et al. (2020) and Wang et al. (2019a, 2019b), respectively. In this paper, we reported the structural determination of new (**1** and **2**) and known (**10** and **13**–**16**) compounds (see Table 2).

2.6. Structural characterization of compounds *1*, *2*, *10*, and *13*–*16*

Compound **1** was obtained as colorless gum with the specific rotation of $[\alpha]_D^{20}$ + 14.29 (c 0.28, CH_3 OH). Compound **1** had a molecular formula of $C_{57}H_{88}O_{22}$ as determined by the negative HRESIMS at *m/z* 1123.5679 $[M-H]^-$ and 1159.5445 $[M+Cl]^-$, with different values of 1.38 and 1.40 ppm compared to those of the calculated quasi-molecular ion peaks at $[M-H]^-$ (1123.5694 Da) and $[M+Cl]^-$ (1159.5461 Da). The chemical structure of **1** was fully discussed based on the NMR analysis. In the ^1H NMR spectrum (in pyridine d_5), resonances at the low field region of 5.0 to 8.5 ppm corresponded to characteristic protons of a moiety of *trans-p*-hydroxyphenylacryloyl (*p*-coumaroyl) at δ_H 7.62 (2H, d, J = 8.4 Hz, H-2‴′, 6‴′), 7.18 (2H, d, J = 8.4 Hz, H-3‴′, 5‴′), 8.00 (1H, d, J = 15.6 Hz, H-7‴′), and 6.73 (1H, d, J = 15.6 Hz, H-8‴′). In addition, resonance signals at δ_H 0.19 and 0.79 (each 1H, brs) of methylene (CH_2) should be attributed to characteristic cyclopropane methylene protons (CH_2-19), the specific three-member ring

Table 1 The *in vitro* neuroprotective activity assay of the separation intermediates.[a]

Fragments		H_2O_2 damage model
	Cell viability and deviation	
Blank	100.00 ± 8.79	–
Model		61.98 ± 3.52###
GSJ-M		63.80 ± 7.88
GSJ-M-A		53.44 ± 6.54*
GSJ-M-B		77.22 ± 6.74*
GSJ-M-C		77.10 ± 8.21*
GSJ-M-D		59.25 ± 6.33*

[a] Final sample concentration:10^{-3} M; ###p < 0.001, *p < 0.05.

Table 2 the ^{1}H and ^{13}C NMR spectroscopic data of compounds **1** and **2**.[a]

No.	^{1}H NMR, δ in ppm, coupling constant in Hz		^{13}C NMR	
	1	2	1	2
1	2.06, 1.15(each 1H, m)	1.26,0.94 (each 1H, m)	32.60	31.62
2	2.54,2.03 (each 1H, m)	2.35, 1.84 (each 1H, m)	29.97	29.76
3	3.67 (1H,dd, 12.0, 4.8)	3.63 (1H, dd, 11.4, 4.8)	89.41	90.81
4	–	–	44.86	44.12
5	1.39 (1H, m)	1.18 (1H, m)	48.27	47.38
6	1.68, 1.28 (each 1H, m)	1.46,1.38 (each 1H, m)	22.71	21.54
7	1.32, 1.27 (each 1H, m)	0.87 (2H, m)	29.37	26.36
8	1.39(1H, m)	1.23 (1H, m)	48.38	48.22
11	1.64, 1.88 (each 1H, m)	1.38, 0.83 (each 1H, m)	26.67	26.35
12	1.24, 1.16(each 1H, m)	1.11(2H, m)	35.63	35.59
13	–	–	45.36	45.32
14	–	–	48.74	48.64
15	1.67 (2H,m)	1.51 (2H,m)	33.07	33.10
16	2.14,1.49 (each 1H, m)	2.04, 1.40 (each 1H, m)	28.16	28.22
17	1.71(1H, m)	1.57 (1H, m)	53.52	53.45
18	0.93 (3H, s)	0.85 (3H, s)	18.41	18.23
19	0.22, 0.79 (each 1H, brs)	0.09, 0.01 (each 1H, brs)	29.34	29.53
20	1.62 (1H, m)	1.97 (1H, m)	32.52	32.46
21	1.10 (3H, d, 6.0)	1.00 (3H, d, 6.0)	18.05	18.06
22	2.43, 1.30 (each 1H, m)	2.33 (1H, dd, 14.4, 11.4); 1.21 (1H, m)	42.66	42.67
23	4.26 (1H, m)	4.15 (1H, m)	67.45	67.43
24	3.80 (1H, brs)	3.67 (1H, brs)	93.66	93.72
25	–	–	73.17	73.21
26	1.76(3H, s)	1.63 (3H, s)	26.26	26.26
27	1.59(3H, s)	1.47 (3H, s)	26.76	26.68
28	0.93 (3H, s)	0.78 (3H, s)	19.41	19.27
29	0.90 (3H, s)	1.23 (3H, s)	20.31	20.51
30	4.68(1H, d, 10.2); 4.28(1H, m)	4.31, 3.30 (each 1H, brs)	70.84	63.51
1′	4.96 (1H, d,7.8) **3-1**[b]	4.67 (1H, d,7.8) **3-1**[b]	107.16	104.2
2′	4.12(1H, m)	4.02(1H, m)	75.77	80.11
3′	4.25 (1H, m)	3.68(1H, m)	78.35	76.27
4′	4.18(1H, m)	4.17 (1H, m)	71.25	71.45
5′	3.98 (1H, m)	4.10 (1H, m)	78.21	78.29
6′	4.54, 4.38 (each 1H, m)	4.36, 4.16 (each 1H, m)	62.48	62.09
1″	5.20(1H, d, 7.8) **24-1**[d]	5.05(1H, d,7.8) **3-2**[e]	106.80	104.66
2″	4.10(1H, m)	3.96 (1H, m)	75.30	74.67
3″	4.27 (1H, m)	4.24(1H, m)	78.32	78.32
4″	3.97(1H, m)	4.17(1H, m)	71.57	71.48
5″	4.17 (1H, m)	3.84(1H, m)	78.01	78.30
6″	5.08 (2H, m)	4.40, 4.27 (each 1H, m)	64.38	62.07
1‴	4.78(1H, d,7.8) **30-1**[f]	5.03(1H, d,7.8) **24-1**[d]	105.41	106.79
2‴	4.01(1H, m)	4.16 (1H, m)	75.34	80.43
3‴	4.18 (1H, m)	4.15(1H, m)	78.31	76.73
4‴	4.18(1H, m)	4.18(1H, m)	71.65	71.57
5‴	3.79(1H, m)	4.01(1H, m)	77.89	78.03
6‴	4.46 (2H, m)	4.34, 4.26 (each 1H, m)	62.58	61.65
1⁗	–	5.40(1H, d,7.8) **24-2**[e]	133.66	104.11
2⁗	7.62 (1H, d, 8.4)	3.96 (1H, m)	130.53	75.83
3⁗	7.18 (1H, d, 8.4)	4.25(1H, m)	116.66	78.31
4⁗	–	4.20(1H, m)	161.26	71.60
5⁗	7.18 (1H, d, 8.4)	4.01(1H, m)	116.66	78.10
6⁗	7.62 (1H, d, 8.4)	4.40, 4.27 (each 1H, m)	130.53	61.47
7⁗	8.00 (1H, d, 15.6)	–	145.08	–
8⁗	6.73 (1H, d, 15.6)	–	115.05	–
9⁗	–	–	167.27	–

[a] NMR data (δ) was measured at 600 MHz for ^{1}H and 150 ppm for ^{13}C in pyridine d_5. Proton coupling constants (J) in Hz are given in parentheses. The assignments were based on DEPT, ^{1}H-^{1}H COSY, gHMQC and HMBC experiments; [b,c] the first and second glycosyl groups that located at C-3; [d,e] the first and second glycosyl groups that located at C-24; [f] the glycosyl group connected with C-30.

of cycloartane triterpenoid that has been previously discovered in *A. ruprechtii* (Wang et al., 2020). This speculation was supported by the existence of five single methyl signals at 0.93 (3H, s), 1.76 (3H, s), 1.59 (3H, s), 0.93 (3H, s), and 0.90 (3H, s) and a doublet one at 1.10 (3H, d, 6.0). The ^{13}C and DEPT NMR data showed that **1** has other 24 carbons of the cycloartane triterpenoid skeleton, including 10 methylene, 7 methine, and 6 quaternary carbon. Furthermore, three glycosyl groups were supported by anomeric protons at δ_H 4.96 (1H, d, 7.8), 5.20 (1H, d, 7.8), and 4.78 (1H, d, 7.8) and corresponding carbons at 107.16, 106.80, and 105.41 ppm.

By comparing the NMR data of **1** to that of 3*β*,30-*O*-*β*-D-glucopyranosyl-24-*O*-[*β*-D-glucopyranosyl-(1 → 2)-*O*-*β*-D-glucopyranosyl]-7*β*,25-dihydroxycycloartane (aspleniumside A) (Wang et al., 2020), reported in our previous studies, we found that O-CH-7 in aspleniumside A was reduced to a CH_2 group in **1** and CH_2-23 in aspleniumside A was oxidized to CH-OH. These results were also supported by 2D NMR spectra including ^1H-^1H COSY, qHMQC, and heteronuclear multiple bond correlation (HMBC) (Fig. 2). In the ^1H-^1H COSY, the cross-peaks of H_2-15/H_2-16/H-17/H-20(H_3-21)/H_2-22/H-23(O)/H-24(O) verified the existence of CH(OH)-23. The glycosyl groups were shown to connect with C-3, C-24, and C-30, respectively, based on HMBC correlations of H-1′ with C-3, H-1″ with C-24, and H-1‴ with C-30. Additionally, the HMBC correlation of H-6″ to C-9‴′ indicated that the *p*-coumaroyl moiety was connected with C-6″ forming an ester linkage. The glycosyl groups in **1** were determined by acid-catalyzed hydrolysis. The co-TLC of the hydrolysate with a positive standard of D-glycoside in the development solvents of $CHCl_3$:CH_3OH:H_2O of 7:3:1 suggested that all glycosyl groups in **1** were *β*-D-glucopyranosyl as other cycloartane-triterpenoid saponins that were previously isolated in the same species (Li et al., 2010; Li et al., 2008; Li et al., 2006a, 2006b; Wang et al., 2020; Zhang et al., 2008).

The relative configuration of **1** was determined by 2D NOESY analysis (Fig. 2). The correlations of H_2-19 with H2-30 and H-8 with H_3-18 indicated that these protons bear the same orientation. The NOESY correlations of H-3 with H-5, H-5 with H_3-28, and H_3-29 and H_3-28 with H-17 suggested that they were orientated on the other side. Therefore, compound **1** was determined as 3*β*, 30-*O*-*β*-D-glucopyranosyl-24-*O*-[6″-O-*p*-coumaroyl-*β*-D-glucopyranosyl]-23, 25-dihydroxycycloartane, assigned as aspleniumside H.

The physicochemical properties of compound **2** resembled that of **1** as a colorless gum with a specific rotation of $[\alpha]_D^{20}$ + 17.54 (c 0.34, CH_3OH). The molecular formula $C_{54}H_{92}O_{25}$ was deduced by the negative HRESIMS ions at *m/z* 1139.5822 $[M-H]^-$ (calculated as $C_{54}H_{93}O_{25}$ of 1139.5855 Da by a difference of 2.89 ppm) and *m/z* 1175.5596 $[M+H]^-$ (calculated as $C_{54}H_{92}O_{25}Cl$ of 1175.5622 Da by a difference of 2.19 ppm), together with the NMR data (Table 1). The ^1H NMR of **2** was very similar to that of **1** except the lack of a set of signals in the low field corresponding to the *trans*-*p*-hydroxyphenylacryloyl group. The resonance signals at 0.09 and 0.01 (each 1H, brs) were attributed to CH_2 and six CH_3 signals at 0.85 (3H, s), 1.00 (3H, d, 6.0), 1.63 (3H, s), 1.47 (3H, s), 0.78 (3H, s), and 1.23 (3H, s),

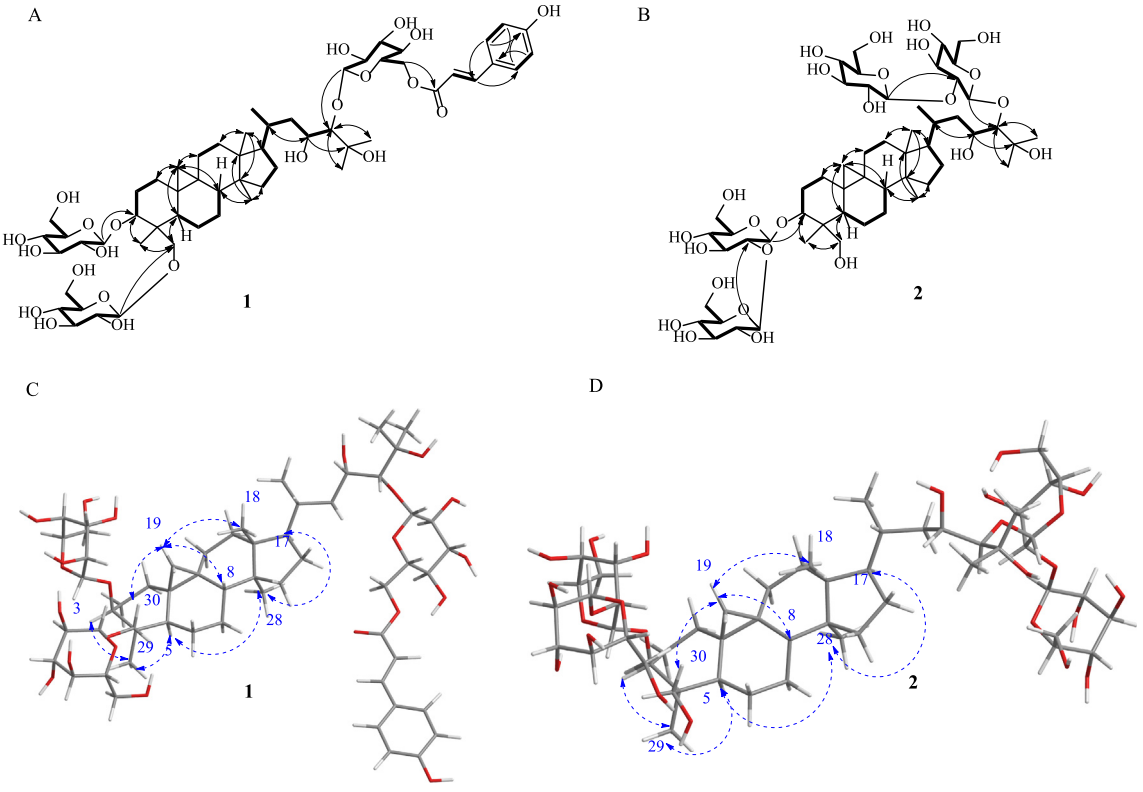

Fig. 2 Key 2D NMR correlations for determining the structures of **1** and **2**. ^1H-^1H COSY (thick bonds) and HMBC correlations (solid arrows) were exhibited as A (**1**) and B (**2**), while the key NOESY correlations (blue dash arrows) were provided as C (**1**) and D (**2**), respectively.

together with the glycosyl signals in a range of 3.0 to 5.5 ppm, indicating that **2** was also a member of cycloartane-triterpenoid saponins. The glycosyl groups were determined as two *β*-D-glucopyranosyl-(1 → 2)-*O*-*β*-D-glucopyranosyl group linked to C-3 and C-24, respectively, by HMBC correlations (Fig. 2) of H-1′ with C-3, H-1″ with C-2′, H-1‴ with C-24, and H-1⁗ with C-2‴. The ^{1}H-^{1}H COSY cross-peaks of H_2-15/H_2-16/H-17/H-20(H_3-21)/H_2-22/H-23/H-24 verified the existence of *O*-bearing carbon of C-23. Therefore, compound **2** was determined as 3*β*, 24-di-*O*-[*β*-D-glucopyranosyl-(1 → 2)-*O*-*β*-D-glucopyranosyl]-23, 25, 30-trihydroxycycloartane, assigned as aspleniumside I.

The known compounds were determined as 10-*O*-acetyl-6-hydroxyadoxoside (**10**) (Su et al., 2005), kaempferol-3-*O*-[(6-*O* -*E*-caffeoyl)-*β*-D-glucopyranosyl]-(1 → 2)-*β*-D-glucopyranosyl-7-*O*-*β*-D-glucopyranoside (**13**) (Fan et al., 2012), kaempferol-3-*O*-[(6-*O*-*p*-coumaroyl)-*β*-D-glucopyranosyl]-(1 → 2)-*β*-D-glucopyranosyl-7-*O*-*β*-D-glucopyranoside (**14**) (Li et al., 2006a, 2006b), kaempferol-3-*O*-[(6-*O*-*E*-feruloyl)-*β*-*D*-glucopyranosyl]-(1 → 2)-*β*-*D*-galacopyranoside (**15**) (Li et al., 2006a, 2006b), and quercetin-3-*O*-[(6-*O*-*E*-feruloyl)-*β*-*D*-glucopyranosyl]-(1 → 2)-*β*-*D*-glucopyranoside (**16**) (Li et al., 2006a, 2006b), by comparison of their NMR data to those in the literature.

2.7. Neuroprotective activity assay of the monomers

The neuroprotective activity of the monomers was determined using H_2O_2-induced damage of SH-SY5Y cell lines as a model at a concentration level of 10^{-5} M. Compounds **10** and **13**–**16** showed protective activities with 1.09 to 1.26 times of cell viability compared to the negative control. Compounds **1** to **7** showed some toxic effects in terms of lower cell viability (Table 3).

Table 3 The *in vitro* neuroprotective activity assay of the separation intermediates.[a]

Fragments		H_2O_2 damage model
	Cell viability and deviation	
blank	100.00 ± 8.79	–
model		61.98 ± 3.52$^{###}$
1		38.82 ± 3.48
2		33.44 ± 7.46*
3		32.22 ± 6.70*
4		47.10 ± 7.21*
5		52.25 ± 4.30*
6		58.43 ± 6.76*
7		54.22 ± 3.30*
8		60.20 ± 3.20*
9		58.24 ± 5.56*
10		56.43 ± 3.14*
11		57.12 ± 4.46*
12		56.24 ± 4.68*
13		56.43 ± 3.14*
14		75.63 ± 5.44*
15		71.61 ± 7.94*
16		66.54 ± 6.32*

[a] Final sample concentration:10^{-3} M; $^{###}p < 0.001$, $^{*}p < 0.05$.

2.8. Cytotoxicity assay

Cytotoxicity effects of compounds **3**–**7** on the tumor cells have previously been reported by our group. Herein, compound **2** exhibited cytotoxic activity against HL-60 and HepG2 cells with the half-maximal inhibitory concentration (IC_{50}) value of 60.24 ± 4.26 and 40.15 ± 2.23 μM, respectively, and > 100 μM for compound **1**, while the positive control of Sorafeni showed cytotoxic activity against HL-60 and HepG2 cells with an IC_{50} value of 10.61 ± 0.43 and 13.43 ± 1.12 μM, respectively, indicating that **2** has a weak anti-tumor activity.

2.9. Docking of compounds *1*–*16* to the N-terminal of the GluN2B protein

The N-terminal of the GluN2B protein has been considered to be the "active pocket" in the literature. In this study, the neuroprotective activity of all monomer compounds was evaluated using the autodocking method. Stable conformation of **1**–**16** was yielded by the Chem3D software using the default MM2 algorithm. The binding effect between small molecular ligands and macromolecular protein was determined by the total score (Table S1). The higher binding scores of **13**–**16** were identical to their *in vitro* neuroprotective activity data, indicating that binding to the GluN2B protein is one of the important mechanisms that should be considered.

Modern medicinal-oriented natural products research has broken numerous difficulties and bottlenecks, especially in the improvement of modern analytical methods and techniques. This has facilitated the establishment of structures of ultra-trace chemical components in natural resources using combined chromatographic analyses, such as HPLC-MS/MS, HPLC-NMR-MS/MS, etc. Several new compounds and skeletons have been discovered and reported (Jiang et al., 2017; Meng et al., 2016; Jiang et al., 2018; Shi et al., 2016; Wu et al., 2019). However, due to the limitation of the number of compounds and the lack of tracking during the isolation progress, systematic evaluation of most important biological activities has been impossible. Therefore, the establishment of novel bioassay-guided techniques in the process of screening bioactive compounds remains a hot topic among organic chemists and pharmacologists.

Traditional Chinese medicines and ancient folk medicine in India and other countries with a long history have been used clinically and proved effective. However, their active and effective chemicals have always been a mystery, attracting scientific attention. Systematically expounding the chemical compositions based on bioactivity evaluation may be advantageous in the discovery of active chemical molecules, hence, saving time and resources during research and development of effective drugs. In this study, the evaluation of neuroprotective activity was employed in the screening of new bioactive compounds in a folk medicine plant, *A. ruprechtii*, leading to the discovery of 16 compounds. We attempted to validate these compounds using the *in vitro* neuroprotective activity evaluation and docking to the "active pocket" of the GluN2B protein that was considered to be related to the neuroprotective activity. This yielded four flavonoid glycosides (**13**–**16**), which exhibited biological activities.

3. Conclusions

Based on neuroprotective activity evaluation, the chemical compositions of a thromboangitis obliterans-treating folk medicine (*A. ruprechtii*) were investigated, leading to the isolation of 16 compounds, including two new cycloartane-triterpenoid saponins (**1** and **2**). Their structures were determined based on the extensive analysis of the NMR data. *In vitro* evaluation demonstrated that compounds **13** to **16** had potential neuroprotective activity against H_2O_2-induced damage in SH-SY5Y cell lines and the higher docking binding scores to the GluN2B protein. Overall, our findings demonstrate the importance of neuroprotective activity evaluation as an effective technique in the characterization of bioactive compounds from medicinal plants.

Contributors' Statement

Extraction and separation: X. Lu, J. Chen, and X. Ma; Cytotoxicity test: D. Zhang; Cell culture: F. Wang; Cell viability assay: F. Wang; Docking experiments: S. Cao; Project supervision: Z. Jiang; Structural analysis: Y. Ke, X. Guo, and H. Liu; NMR spectroscopy: C. Li and X. Wu.

Declaration of Competing Interest

The authors declare that they have no known competing financial interests or personal relationships that could have appeared to influence the work reported in this paper.

Acknowledgements

This work was co-funded by the Key R&D projects in Ningxia province [Grant numbers: 2020BFG02006 and 2019BEB04028); the '2019 Western Light' Program for Scholars in Western China [Grant number: XAB2019AW05); the Scientific Research Start-up Project for Recruitment Talents of North Minzu University in 2019 [Grant number: 113159150]; Jinan innovation team project 2019 [Grant number: 2019GXRC039]; the Natural Science Foundation of Ningxia Province [Grant numbers: 2020AAC03248 and 2020AAC03206]; and the National Natural Science Foundation of China [Grant number: 81603006].

Appendix A. Supplementary matrial

The (-)-HRESIMS, ^{1}H and ^{13}C NMR, DEPT, COSY, gHMQC, HMBC, and NOESY spectra for compounds **1** and **2**; and the ^{1}H and (or) ^{13}C NMR for compounds **10** and **13-16** are provided in Appendix A. Supplementary data to this article can be found online at https://doi.org/10.1016/j.arabjc.2020.10.011.

References

41K of Shenyang College of Pharmacy, 1977. Dilatation of blood vessels and toxicities of Camptosorus sibiricus Rupr. J. Shenyang Pharm. Univ. 7, 34–37.

Caputo, M., Lyles, J.T., Salazar, M.S., Quave, C., 2020. LEGO MINDSTORMS fraction collector: A low-cost tool for a preparative high-performance liquid chromatography system. Anal. Chem. 92, 1687–1690.

Ching, R., 1978. The Chinese fern families and genera: systematic arrangement and historical origin. J. Syst. Evol. 16, 1–19.

Christenhusz, M., Zhang, X.C., Schneider, H., 2011. A linear sequence of extant families and genera of lycophytes and ferns. Phytotaxa 19, 7–54.

Christenhusz, M.J.M., Chase, M.W., 2014. Trends and concepts in fern classification. Ann. Bot. 113, 571–594.

Fan, P., Zhao, L., Hostettmann, K., Lou, H., 2012. Chemical constituents of *Asplenium ruta-muraria* L. Nat. Prod. Lett. 26, 1413–1418.

Hasebe, M., Wolf, P.G., Pryer, K.M., Ueda, K., Ito, M., Sano, R., Gastony, G.J., Yokoyama, J., Manhart, J.R., Murakami, N., Crane, E.H., Haufler, C.H., Hauk, W.D., 1995. Fern phylogeny based on *rbcL* nucleotide sequences. Am. Fern. J. 85, 134–181.

Huang, X.M., Yang, Z.J., Xie, Q., Zhang, Z.K., 2019. Natural products for treating colorectal cancer: a mechanistic review. Biomed. Pharmacother. 117, 109142.

Jamzivar, F., Shams-Ghahfarokhi, M., Khoramizadeh, M., Yousefi, N., Gholami-Shabani, M., Razzaghi-Abyaneh, M., 2019. Unraveling the importance of molecules of natural origin in antifungal drug development through targeting ergosterol biosynthesis pathway. Iran J. Microbiol. 11, 448–459.

Jiang, Z., Lei, X., Chen, M., Jiang, B., Wu, L., Zhang, X., Zheng, Z., Hu, X., You, X., Si, S., Wang, L., Hong, B., 2017. Three structurally-related impurities in norvancomycin drug substance. J. Antibiot (Tokyo) 70, 158–165.

Jiang, Z.B., Ren, W.C., Shi, Y.Y., Li, X.X., Lei, X., Fan, J.H., Zhang, C., Gu, R.J., Wang, L.F., Xie, Y.Y., Hong, B., 2018. Structure-based manual screening and automatic networking for systematically exploring sansanmycin analogues using high-performance liquid chromatography-tandem mass spectroscopy. J. Pharm. Biom. Anal. 158, 94–105.

Li, N., Li, X., Li, X.Z., Zhang, P., Meng, D.L., 2008. New cycloartane glycosides from *Camptosorus Sibiricus* Rupr. J. Asian Nat. Prod. Res. 10, 119–124.

Li, N., Li, X., Meng, D., Wang, J.H., 2006a. Flavonoids from *Camptosorus Sibiricus* Rupr. J Asian Nat. Prod. Res. 8, 167–171.

Li, N., Li, X., Zhang, P., Wang, J.H., 2006b. A new cycloartane glycoside from *Camptosorus sibiricus* Rupr. Nat. Prod. Res. 20, 1041–1045.

Li, N., Xiao, W., Hou, B., Li, X., 2010. New triterpene glycosides from *Camptosorus Sibiricus*. Nat. Prod. Commun. 5, 1557–1560.

Liang, D., Yu, L., Li, N., Liu, Y., Guo, Q., Wang, F., 2017. Chemical constituents of the water extract from *Camptosorus sibiricus* Rupr. J. Shenyang Pharm. Univ. 34, 541–552.

Liang, D., Cheng, Y., Dong, S., Li, N., 2011. Improving effect of total flavonoids from *Camptosorus sibiricus* on rats with thromboangiitis obliterans. Chin. Tradit. Herb. Drugs 26, 481–484.

Lin, Y.X., Ronald, V., 2013. Flora of China. Science Press & the Missouri Botanical Garden Press 2, 16.

Liu, W., Jiang, X., Zu, Y., Yang, Y., Liu, Y., Sun, X., Xu, Z., Ding, H., Zhao, Q., 2020. A comprehensive description of GluN2B-selective N-methyl-D-aspartate (NMDA) receptor antagonists. Eur. J. Med. Chem. 200, 112447.

Meng, X.H., Jiang, Z.B., Zhu, C.G., Guo, Q.L., Xu, C.B., Shi, J.G., 2016. Napelline-type C_{20}-diterpenoid alkaloid iminiums from an aqueous extract of "fu zi": Solvent-/base-/acid-dependent transformation and equilibration between alcohol iminium and aza acetal forms. Chin. Chem. Lett. 27, 993–1003.

Newman, D.J., Cragg, G.M., 2020. Natural products as sources of new drugs over nearly four decades. J. Nat. Prod. 83, 770–803.

Noh, A.S.M., Ismail, C.A.N., 2020. A review on chronic pain in rheumatoid arthritis: a focus on activation of NR2B subunit of N-methyl-D-aspartate receptors. Malays J. Med. Sci. 27, 6–21.

Shi, Y., Jiang, Z., Lei, X., Zhang, N., Cai, Q., Li, Q., Wang, L., Si, S., Xie, Y., Hong, B., 2016. Improving the N-terminal diversity of sansanmycin through mutasynthesis. Microb. Cell. Fact. 15, 1–15.

Su, B.N., Pawlus, A.D., Jung, H.A., Keller, W.J., McLaughlin, J.L., Kinghorn, A.D., 2005. Chemical constituents of the fruits of *Morinda citrifolia* (Noni) and their antioxidant activity. J. Nat. Prod. 68, 592–595.

Treml, J., Gazdová, M., Šmejkal, K., Šudomová, M., Kubatka, P., Hassan, S., 2020. Natural products-derived chemicals: breaking barriers to novel anti-HSV drug development. Viruses 12, 154.

Vieira, M.M., Schmidt, J., Ferreira, J.S., She, K., Oku, S., Mele, M., Santos, A.E., Duarte, C.B., Craig, A.M., Carvalho, A.L., 2016. Multiple domains in the C-terminus of NMDA receptor GluN2B subunit contribute to neuronal death following *in vitro* ischemia. Neurobiol. Dis. 89, 223–234.

Wang, F., Jia, Q., Yuan, Z., Lv, L.Y., Li, M., Jiang, Z.B., Liang, D.L., Zhang, D.Z., 2019a. An anti-inflammatory *C*-stiryl iridoid from *Camptosorus Sibiricus* Rupr. Fitoterapia 134, 378–381.

Wang, F., Jiang, Z.B., Wu, X.L., Liang, D.L., Zhang, N., Li, M., Shi, L., Duan, C.G., Ma, X.L., Zhang, D.Z., 2020. Structural determination and *in vitro* tumor cytotoxicity evaluation of five new cycloartane glycosides from *Asplenium ruprechtii* Sa. Kurata. Bioorg. Chem. 102, 104085.

Wang, X.Y., Li, C.J., Ma, J., Li, C., Chen, F.Y., Wang, N., Shen, C.J., Zhang, D.M., 2019b. Cytotoxic 9,19-cycloartane type triterpenoid glycosides from the roots of *Actaea dahurica*. Phytochemistry 160, 48–55.

Wu, Y., Shao, S., Guo, Q., Xu, C., Xia, H., Zhang, T., Shi, J., 2019. Aconicatisulfonines A and B, analgesic zwitterionic $_{C2}$0-diterpenoid alkaloids with a rearranged atisane skeleton from *Aconitum carmichaelii*. Org. Lett. 21, 6850–6854.

Yang, B., Liu, J., Yang, X., 2012. Research progress in chemical constituents and pharmacological activities of *Camptosorus sibiricus* Rupr. Modern. Chin. Med. 14, 18–22.

Zhang, L., Yu, H., Sun, Y., Lin, X., Chen, B., Tan, C., Cao, G., Wang, Z., 2007. Protective effects of salidroside on hydrogen peroxide-induced apoptosis in SH-SY5Y human neuroblastoma cells. Eur. J. Pharmacol. 564, 18–25.

Zhang, P., Cheng, Y.Y., Ma, Z.J., 2008. New cycloartane glycosides from *Camptosorus sibiricus* Rupr. J. Asian Nat. Prod. Res. 10, 1069–1074.

Zhou, X., Ding, Q., Chen, Z., Yun, H., Wang, H., 2013. Involvement of the GluN2A and GluN2B subunits in synaptic and extrasynaptic N-methyl-D-aspartate receptor function and neuronal excitotoxicity. J. Biol. Chem. 288, 24151–24159.